Supplementary Information

Thiolene and SIFEL-based Microfluidic Platforms for Liquid-Liquid Extraction

*Sachit Goyal, Amit V. Desai, Robert W. Lewis, David R. Ranganathan, Hairong Li, Dexing Zeng, David E. Reichert, Paul J. A. Kenis**

1. Materials

All the chemicals were used as received, unless specified. Thiolene-based optical adhesive, NOA 81, was purchased from Norland Products. RTV 615 A/B poly(dimethyl siloxane) or PDMS was purchased from General Electric Company (Waterford, NY). SU-8 2050 was purchased from MicroChem Corporation (Newton, MA). SPR220-7 was purchased from Shipley. (Tridecafluoro-1,1,2,2- tetrahydrooctyl) trichlorosilane and 1H,1H,2H,2H-perfluorodecyltrichlorosilane or (Heptadecafluoro-1,1,2,2-tetrahydrodecyl)trichlorosilane, *i.e.*, FDTS were purchased from Gelest, Inc. (Morrisville, PA). SIFEL X-71 8115 A/B was purchased from Shin-Etsu Silicones of America (Akron, OH). 3M^{TM} Novec^{TM} EGC 1700 Electronic Coating and 3M^{TM} Novec^{TM} DL 7100 Engineering Fluid was purchased from 3M (St. Paul, MN). De-ionized water (DI-H2O) was produced using a Millipore Milli-Q water system. Caffeine, n-octanol, phosphate buffer (PBS, pH 7.4), isooctane, isopropanol, and toluene were purchased from Sigma Aldrich (St. Louis, MO). $^{64}Cu^{2+}$ in 0.1M HCl solution was produced at Washington University School of Medicine and obtained through the Radionuclide Resource for Cancer Applications. 2-Hydroxy-4-n-octyloxybenzophenone oxime (HOBO) was synthesized at the Washington University School of Medicine. [1]

2. Surface functionalization for thiolene–glass microfluidic platform

The procedure for surface functionalization was adapted from a previous research [2] and the setup is shown in Fig. S1. Isooctane solution was first flowed into the microchannels at 30 μL/min for 15 min. to wet the microchannels. To functionalize the surfaces, the isooctane solution was then replaced with 1 % (wt./wt.) solution of FDTS in isooctane, and flowed into either one or both the inlets at 30 μL/min for 15 min. After 15 min. of incubation, excess FDTS was removed by flushing the channel first with isooctane and then isopropanol, each for 20 min at 30 μL/min. The microfluidic platform was dried overnight at room temperature.

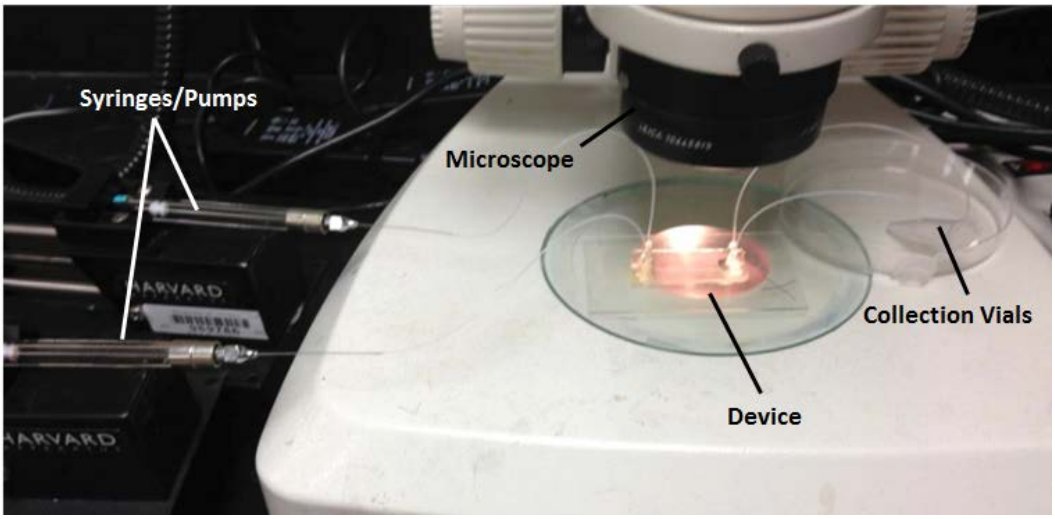

Fig. S1 Experimental setup that includes two airtight syringes mounted on computer-operated pumps, which are used to co-flow solutions into the microfluidic platform (labelled device in figure). Collection vials were placed at the end of the outlet tubing. This setup is used for surface functionalization, study of interface stability and phase separation, and determining lipophilicity of caffeine.

3. Contact angle measurements

The two-phase contact angles were measured for water-toluene and water-octanol on untreated glass (cover slip), thiolene (spin-coated on cover slip) and SIFEL (thin layer spin-coated on cover slip) substrates, and thiolene and glass substrates treated with FDTS. The substrates were cleaned with isopropanol and water. In case of treated surfaces, the glass and

thiolene substrates were immersed in 1% FDTS in isooctane solution for different periods. Small pieces of the substrate were put at the bottom of a 3.5 mL UV-vis glass cuvette (Azzota, G104, 340-2500 nm). Toluene or octanol was filled in the cuvette and a water drop introduced on the surface with a pipette. Images of the droplet wetting the substrate was captured using a Canon EOS Rebel T3 digital SLR camera equipped with a compact Macro-Lens EF 50mm 1:2.5. The contact angle was then measured using the "angle" tool in Image J 1.46s.

4. Experimental setup to study interface stability and phase separation

The experimental setup comprised of the microfluidic platform, 1 mL gastight glass syringes (Model 1001, Hamilton Co.) with needles (B-D 26G), 1.7 mL polypropylene micro-centrifuge tubes with caps (United Lab Plastics), syringe pumps (Catalog No. 70-2225 Harvard Apparatus), and a stereomicroscope (Leica MZ 12.5) with Micrometrics SE (Micrometrics) imaging software (Fig. S1). Syringe pumps were operated by Hyper Terminal software in Windows to control the flow rate of each stream in the microfluidic platform. Communication between the software and the syringe pump drivers was facilitated through a serial connection. The liquid-liquid interface along the length of the microfluidic platform and the phase separation was observed periodically at different flow rates using the stereomicroscope.

5. Experiment to determine lipophilicity of caffeine

5.1 HPLC Analysis

5.1.1 Preparation of calibration solutions for caffeine concentration

Reference stock solutions of caffeine were prepared in phosphate buffer and n-octanol (0.5, 1, 2, 3, 4, 5 mM of caffeine dissolved in octanol and phosphate buffer). A 20 μL aliquot of each caffeine sample was transferred to a HPLC vial with vial inserts (Agilent Technologies). The samples were analyzed using high performance liquid chromatography (HPLC) to prepare

standard concentration calibration curves that were further employed as reference for quantifying caffeine extraction efficiency from one phase to the other.

5.1.2 Analysis of samples for quantifying caffeine concentration

At the end of each reaction run, a 20 μL aliquot of caffeine sample in n-octanol and PBS collected in a micro centrifuge tube was transferred to HPLC vials with vial inserts (Agilent Technologies). The chromatographic separations were performed using Agilent Technologies, 1100 series HPLC value system arranged with an isocratic pump, manual injector, and variable wavelength detector. A Phenomenex™ HPLC column (Luna 5u C18 (2) 100A 50x2 00B-4252-B0) was used as the stationary phase. The components were separated isocratically with a mobile phase that consists of a gradient of 0.1% formic acid in water and 0.1 % formic acid in acetonitrile. We started with 95% aqueous phase, ramped it down to 5% in 10 minutes, held it at 5% for 3 minutes, and finally ramped it up to 95% in 1 minute. The solutions were flowed at 0.5 mL/min. The analysis was carried out at ambient temperature with an injection volume of 1 μL. The UV detector was set at 274 nm and the elution time was 15 minutes.

5.2 Procedure for determining the lipophilicity of caffeine

Caffeine solution (1 mM) prepared in n-octanol and phosphate buffer solution was co-flowed into the microfluidic platform after functionalizing the microfluidic platform with FDTS (Fig. S1). The flow rates of the n-octanol and buffer solutions were adjusted to 10 μL/min and 45 μL/min, respectively to achieve a stable aqueous-organic interface throughout the length of the microfluidic platform and clean phase separation (minimal leakage) at the exit. The contact time was determined by dividing the length of the microchannel (10 mm) by the linear velocity (flow rate/cross section area of the microchannel) of the slower moving phase (usually the n-

octanol phase in the lipophilicity experiment), as that is the total time for which octanol phase is in contact with the aqueous buffer phase. The contact time for each run was determined to be 0.3 seconds based on our calculations (linear velocity: (10 µl/min)/(200µm*50 µm) = 0.33m/s; contact time: 10mm/0.33m/s = 0.3s). After the experiment, solution at each outlet was collected in 1.7 mL polypropylene micro-centrifuge tubes. The collected samples from Run1 were co-flowed again into the microfluidic platform in a subsequent experiment (Run 2). Similarly, samples from Run 2 were co-flowed into the microfluidic platform for future runs. A 20-µL aliquot of each sample was collected at the end of each run and analyzed using HPLC to determine the extraction efficiency of caffeine from octanol into phosphate buffer. Each experiment was repeated 4 times.

6. Experiment for extraction of radioactive copper

The activity of radioactive copper (64-Cu) was measured for all samples with the radioisotope dose calibrator (Capintec CRC-712M). At the beginning of the experiment, the activity of $^{64}Cu^{2+}$ solutions in 0.1M HCl was measured prior to injection into the microfluidic platform, which typically corresponded to about few pico-molar concentration of copper. These low concentration values for radioactive copper are typical due to the regulations on distribution and handling of radioactive copper [3]. Then, the copper solution and 10 µM HOBO in toluene solution were co-flowed into the microfluidic platform at 20 and 35 µL/min, respectively, for 10 minutes. At the end of each run, the activity of the samples collected in the micro-centrifuge tubes (toluene as well as the aqueous stream) along with residual activity in the microfluidic platform and tubing was measured. The extraction efficiency of the microfluidic platform was calculated using the activity values of the solutions prior to injection and post-injection, and residual solutions.

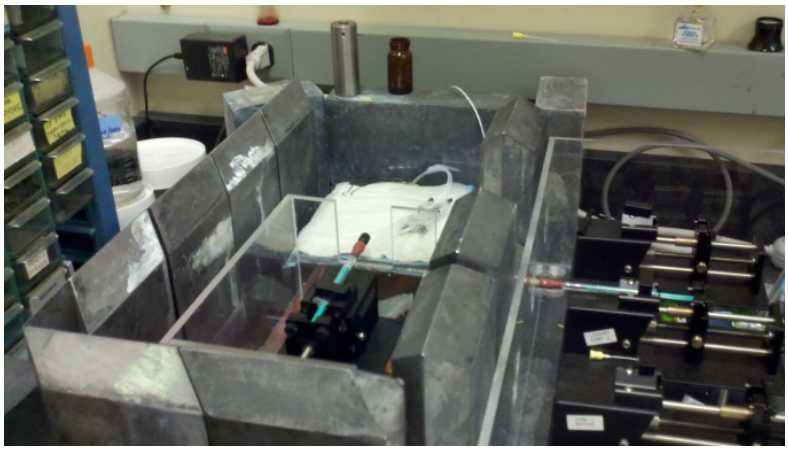

Fig. S2 Experimental setup that includes two airtight syringes mounted on computer-operated pumps, which are used to co-flow solutions into the microfluidic platform. The syringe for radioactive copper is shielded by lead bricks to minimize exposure to ionizing radiations. Collection vials were placed at the end of the outlet tubing.

7. Derivation of expression for maximum extraction length

The expression for maximum extraction length is derived by balancing the laplace pressure and the hydrodynamic pressure difference between the two phases [4, 5] (Fig. 3(b)).

The laplace pressure ($P_{laplace}$) is given by [4]

$$P_{laplace} = \frac{2\gamma \sin(\theta_{contact} - 90)}{h}, \qquad (1)$$

where

γ : surface tension between the two phases

$\theta_{contact}$: contact angle between the two phases

h : height of microchannel.

The hydrodynamic pressure drop (P_{hydro}) for a channel with rectangular cross-section is given by the following expression:

$$P_{hydro} = Q\overline{R}L, \qquad (2)$$

where

Q: volumetric flow rate

$\overline{R}$: hydrodynamic resistance per unit length of channel

L: length of the channel over which pressure drop is being calculated.

The difference in the hydrodynamic pressures for the two phases can be estimated as follows:

$$\begin{aligned} P_{aq}^{total} &= Q_{aq}\overline{R_{aq}}L_{ext} + P_{aq}^{outlet} \\ P_{org}^{total} &= Q_{org}\overline{R_{org}}L_{ext} + P_{org}^{outlet} \\ \Delta P_{flow} &= P_{aq}^{total} - P_{org}^{total} = L_{ext}\left(Q_{aq}\overline{R_{aq}} - Q_{org}\overline{R_{org}}\right) + \Delta P_{outlet} \\ \text{where } \Delta P_{outlet} &= P_{aq}^{outlet} - P_{org}^{outlet} \end{aligned} \qquad (3)$$

where

P^{total}: total pressure drop across the microfluidic platform

P^{outlet}: pressure drop across the outlet channel and tubing

L_{ext}: maximum extraction length of the microchannel

and the subscripts *aq* and *org* indicate the aqueous and organic phases, respectively.

The expression for L_{ext} can be derived by equating $P_{laplace}$ and ΔP_{flow} (Eq. (1) and (3)) and is given by

$$L_{ext} = \frac{\frac{2\gamma\sin\left(\theta_{contact} - 90\right)}{h} - \Delta P_{outlet}}{Q_{aq}\overline{R_{aq-ext}} - Q_{org}\overline{R_{org-ext}}}, \qquad (4)$$

where

ΔP_{outlet} : difference between the hydrodynamic pressures in the outlets

Q_{aq} and Q_{org} : flow rates of the aqueous and organic phases, respectively

$\overline{R_{aq-ext}}$ and $\overline{R_{org-ext}}$: hydrodynamic resistance of the microchannel per unit length in the extraction zone of the aqueous and organic phases, respectively.

8. Derivation of expression for maximum extraction efficiency

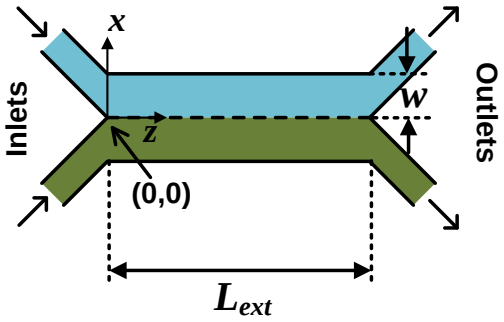

Fig. S3 Schematic illustration of the microfluidic platform for deriving expression for maximum extraction efficiency.

To derive an expression for maximum extraction efficiency, we assume that the extraction is limited by diffusion of the chemical entity in the blue phase towards the interface. Since we do not account for kinetics of extraction at the interface, the derived expression is for the maximum extraction efficiency. The extraction is modeled as 1-D diffusion process along the *x* direction using Fick's law as follows:

$$\frac{\partial C}{\partial t} = D_{ext}\frac{\partial^2 C}{\partial x^2}, \qquad (5)$$

where

D_{ext}: diffusivity of the extracting species

C: concentration of the extracting species.

Assuming steady-state laminar flow, we transform the time coordinate (t) to axial coordinate (z), so that the concentration is a function of x and z. The diffusion equation (Eq. (5)) is given by

$$\frac{\partial C(x,z)}{\partial z} = \frac{D_{ext}}{U_{ext}}\frac{\partial^2 C(x,z)}{\partial x^2}, \qquad (6)$$

U_{ext} : linear velocity of the phase in which the extracting species is diffusing towards the interface.

The boundary conditions for the partial differential equations are given by

$C(x/0,0) = C_0$ concentration is C_0 when the solution enters the channel, except at origin

$C(0,z) = 0$ concentration is zero at interface, as the process is diffusion - limited , (7)

$\frac{\partial C(w,z)}{\partial x} = 0$ flux is zero at the microchannel wall

where

C_0 : initial concentration

w : half-width of microchannel.

We derive an expression for concentration by solving the partial differential equation (Eq. (6)) subject to boundary conditions (Eq. (7)), and the expression is given by

$$C(x,z) = C_0\left[\sum_{n=1,3,5,\ldots} \exp^{-\lambda_n{}^2 k^2 z} \sin\left(\frac{n\pi}{2}x\right)\right], \qquad (8)$$

where $k = \sqrt{\frac{D_{ext}}{U_{ext}}}$ and $\lambda_n = \frac{n\pi}{2w}$.

To estimate the extraction efficiency, we derive an expression for total concentration (C_{total}) in the blue phase, and the expression is given by

$$C_{total} = \int_0^{L_{ext}} \int_0^{w} \sum_{n=1,3,5,\ldots} \exp^{-\lambda_n{}^2 k^2 z} \sin\left(\frac{n\pi}{2}x\right) dxdz\,. \qquad (9)$$

Using Eq. (9), the extraction efficiency (Ψ) is given by

$$\Psi = 1 - \frac{C_{total}}{C_0 L_{ext} w}$$

$$\Psi = 1 - \left[\frac{1}{L_{ext} w}\int_0^{L_{ext}} \int_0^{w} \sum_{n=1,3,5,\ldots} \exp^{-\lambda_n{}^2 k^2 z} \sin\left(\frac{n\pi}{2}x\right) dxdz\right] \qquad (10).$$

9. Generation of design maps

To generate the design maps, we first simplify the expression for L_{ext} (Eq. (4)). We assume the hydrodynamic resistance for rectangular channel is given by [6]

$$\overline{R} = \alpha \frac{\eta}{A^2}$$
$$\overline{C} = \frac{\overline{P}^2}{A}; A = wh; \overline{P} = 2(w+h); \alpha = \frac{22}{7}\overline{C} - \frac{65}{3} \quad . \qquad (11)$$

We assume that the ratio of aqueous to organic flow rates is correlated to the ratio of viscosities, so that the interface is positioned at the center, and this correlation is given by [7]

$$\frac{Q_{aq}}{Q_{org}} = \left(\frac{\eta_{aq}}{\eta_{org}}\right)^{-0.76} \quad . \qquad (12)$$

By substituting Eq. (11) and (12) in Eq. (4), we derive a simplified expression for L_{ext} that we use to generate the design maps in Fig. 4(a) in the main text:

$$L_{ext} = \frac{2\gamma \sin(\theta_{contact} - 90)}{\frac{\alpha}{w^2 h} Q_{aq} \eta_{aq} \left[1 - \left(\frac{\eta_{org}}{\eta_{aq}}\right)^{0.34}\right]}. \qquad (13)$$

The interfacial surface tension for water-toluene is 37.1 mN/m [8]. The contact angle was assumed to be 132°, which was estimated using our contact-angle measurements. The dynamic viscosity of aqueous solution was assumed to be that of 0.1 M HCl as 1.28 mPa-s [9], while for toluene it was assumed to be 0.59 mPa-s (Wikipedia). The diffusivity of copper in 0.1 M HCl was estimated using the Wilke-Chang equation [10] as 1.32×10^{-9} m^2/s. The channel height was fixed at 50 μm.

10. Explanation for improved phase separation in uniformly functionalized surfaces compared to partially functionalized surfaces

We observed that the phase separation in a thiolene-glass microreactor, where all the surfaces (especially the top and bottom surface being contacted by the liquid-liquid interface) are functionalized by FDTS (uniformly functionalized surfaces), is better than in a reactor with

partial functionalization. The reason for this counter-intuitive observation is that perfect partial functionalization is challenging to achieve due to mixing of the functionalization species (FDTS in this case), due to a gradient of wetting behavior (instead of a sharp boundary) at the liquid-liquid interface (**Fig. S4**). This gradient is a result of the diffusion of FDTS molecules from one isooctane solution to the pure isooctane solution. Hence, a concentration gradient is present at the interface that causes a gradient in the functionalized surfaces at the liquid-liquid interface, and consequently a gradient in the wetting behavior. This wettability gradient at the ends of the microchannel leads to instabilities in phase separation during exit. In case of a fully functionalized microreactor, the gradient is not present, and hence the phase separation is better than that in the partially functionalized reactor. To summarize, ideally a partially functionalized reactor should lead to better phase separation than a fully functionalized reactor. However, in reality, the mixing of the pure and concentrated stream (containing silane) at the interface results in formation of a silane gradient, and hence a wettability gradient, which causes poorer phase separation. This speculation is validated to some extend by very small leakage (<5%) in the untreated SIFEL microreactor, where all the surfaces are similar, and hence the interface wets the contacting surfaces almost identically.

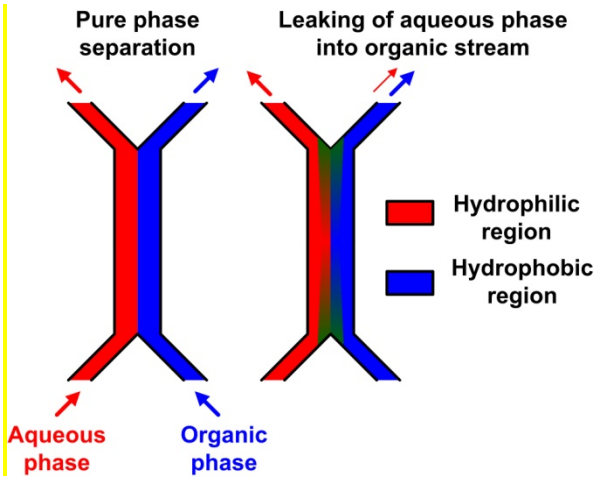

Fig. S4 Schematic illustration of wettability gradient arising during partial functionalization. Image on left shows perfect partial functionalization, where the hydrophilic and hydrophobic regions are separated by a sharp boundary. In this case the phase separation is pure. In reality, the mixing of the streams at the interface during functionalization leads to a gradient of the functionalization molecules, and consequently a gradient in the wetting behaviour. This gradient causes instabilities during exit of the two phases, and hence leakage of one phase into other (*e.g.*, the aqueous phase leaks into the organic phase).

11. Corroboration of efficiency values for copper extraction experiments between experimental results and analytical predictions

We observed that the radioactive Cu-64 was extracted from the aqueous phase to the organic phase containing HOBO with very high efficiency, often exceeding 95%. To obtain estimates using analytical modeling, we make several assumptions about the extraction process to simplify the calculations. The rate of the extraction process for metal ions by an extractant is typically determined by the rates for the following three main steps: (1) mass transfer of metal species from aqueous bulk to the interface between the aqueous and organic phases, (2) complex-formation reaction of the metal species with the extractant at the interface, and (3) mass transfer of formed extracted complex from the interface to the organic bulk [11]. In the copper extraction experiments reported in this paper, firstly, the concentration of HOBO is almost six orders higher than that of copper, and hence an excess of extractant is always present at the interface. Secondly, the overall concentration of HOBO is low (10 μM) compared to typical values in metal extraction experiments [11, 12], which should not significantly affect the diffusion of the extracted complex away from the interface. For these two reasons, we assume that step 3, mass transfer of extracted complex, is not a rate-limiting step. As the concentration of HOBO is very high compared to copper, we assume that the rate for step 2, the metal complexation reaction, is very high, and hence is not a rate-limiting step. To validate this assumption, we performed finite element analysis simulations (using COMSOL) to model the

extraction process comprising of steps 1 and 2. For the copper extraction via HOBO in a water-toluene system, we used the parameter values mentioned in section 9. The complexation rate was estimated using previously reported equations of rate constants [13]. We compared the values for extraction efficiency obtained using simulations to the prediction from analytical modeling, where we assume the rate of the extraction process is limited by the diffusion of the metal species to the interface. We observed that values obtained using simulations and analytical modeling was within 10%, which validates our assumption that the extraction process is diffusion-limited. Note that this assumption is applicable to the copper extraction reported here, and may not necessarily translate to all metal extraction processes. However, this assumption simplifies the calculations and enables us to obtain estimates and identify trends for extraction efficiency, which is useful for design of the microfluidic platform and operating conditions.

References

[1] X.-J. Li, C. Feng, C.-Y. Li and W. Chen, The synthesis of extractant 2-hydroxy-5-nonylacetophenone oxime, Tianjin Huagong 21 (2007) 21-22.

[2] H. Gu, M. H. G. Duits and F. Mugele, A hybrid microfluidic chip with electrowetting functionality using ultraviolet (UV)-curable polymer, Lab on a Chip 10 (2010) 1550-1556.

[3] D. W. McCarthy, R. E. Shefer, R. E. Klinkowstein, L. A. Bass, W. H. Margeneau, C. S. Cutler, C. J. Anderson and M. J. Welch, Efficient production of high specific activity 64Cu using a biomedical cyclotron, Nuclear Medicine and Biology 24 (1997) 35-43.

[4] A. Aota, K. Mawatari and T. Kitamori, Parallel multiphase microflows: fundamental physics, stabilization methods and applications, Lab on a Chip 9 (2009) 2470-2476.

[5] J. Berthier, V.-M. Tran, F. Mittler and N. Sarrut, The physics of a coflow micro-extractor: Interface stability and optimal extraction length, Sensors and Actuators A: Physical 149 (2009) 56-64.

[6] N. A. Mortensen, F. Okkels and H. Bruus, Reexamination of Hagen-Poiseuille flow: Shape dependence of the hydraulic resistance in microchannels, Physical Review E 71 (2005) 057301.

[7] A. Pohar, M. Lakner and I. Plazl, Parallel flow of immiscible liquids in a microreactor: modeling and experimental study, Microfluidics and Nanofluidics 12 (2012) 307-316.

[8] J. Saien and S. Akbari, Interfacial Tension of Toluene + Water + Sodium Dodecyl Sulfate from (20 to 50) °C and pH between 4 and 9, Journal of Chemical & Engineering Data 51 (2006) 1832-1835.

[9] E. Nishikata, T. Ishii and T. Ohta, Viscosities of aqueous hydrochloric acid solutions, and densities and viscosities of aqueous hydroiodic acid solutions, Journal of Chemical & Engineering Data 26 (1981) 254-256.
[10] C. R. Wilke and P. Chang, Correlation of diffusion coefficients in dilute solutions, AIChE Journal 1 (1955) 264-270.
[11] E. Kamio, H. Miura, M. Matsumoto and K. Kondo, Extraction Mechanism of Metal Ions on the Interface between Aqueous and Organic Phases at a High Concentration of Organophosphorus Extractant, Industrial & Engineering Chemistry Research 45 (2005) 1105-1112.
[12] M. A. Hughes and P. K. Kuipa, Kinetics and Mechanism of Copper Extraction with Dialkylphosphoric Acids and Hydroxyoximes Studied by a Rotating Diffusion Cell, Industrial & Engineering Chemistry Research 35 (1996) 1976-1984.
[13] Y. Baba, M. Iwakuma and H. Nagami, Extraction Mechanism for Copper(II) with 2-Hydroxy-4-n-octyloxybenzophenone Oxime, Industrial & Engineering Chemistry Research 41 (2002) 5835-5841.